

The effects of geological heterogeneities and piezometric fluctuations on groundwater flow and chemistry in a hard-rock aquifer, southern India

Jerome Perrin · Shakeel Ahmed · Daniel Hunkeler

Abstract Crystalline aquifers of semi-arid southern India represent a vital water resource for farming communities. A field study is described that characterizes the hydrodynamic functioning of intensively exploited crystalline aquifers at local scale based on detailed well monitoring during one hydrological year. The main results show large water-table fluctuations caused by monsoon recharge and pumping, high spatial variability in well discharges, and a decrease of well yields as the water table decreases. Groundwater chemistry is also spatially variable with the existence of aquifer compartments within which mixing occurs. The observed variability and compartmentalization is explained by geological heterogeneities which play a major role in controlling groundwater flow and connectivity in the aquifer. The position of the water table within the fracture network will determine the degree of connectivity between aquifer compartments and well discharge. The presented aquifer conceptual model suggests several consequences: (1) over-exploitation leads to a drop in well discharge, (2) intensive pumping may contribute to the hydraulic containment of contaminants, (3) groundwater quality is highly variable even at local scale, (4) geological discontinuities may be used to assist

in the location of drinking-supply wells, (5) modeling should integrate threshold effects due to water-table fluctuations.

Keywords Crystalline rocks · Heterogeneity · India · Discontinuity · Conceptual model

Introduction

Crystalline (or hard-rock) aquifers constitute an increasingly important water resource especially in semi-arid regions such as parts of Africa, SE Asia and South America (Gustafson and Krásný 1994). These aquifers are quite modest in terms of yield and storage but they have a proven capability to sustain domestic water supply to rural communities in many regions as well as provide irrigation water for crops that sustain the rural economy.

In southern India, exponential increase in the use of this water resource, especially for irrigation, has led to widespread aquifer over-exploitation and groundwater quality deterioration (e.g., Maréchal et al. 2006; Zaidi et al. 2007; Reddy et al. 2009; Dewandel et al. 2010; Perrin et al. 2011). Therefore there is a need for in-depth understanding of flow and transport processes in these complex aquifer systems (e.g., quantitative evaluation of the resource, preservation of the quality, vulnerability assessment).

Hydrogeological studies on hard-rock aquifers have focused on their structure and link with weathering processes (e.g., Jones 1985; Acworth 1987; Wright 1992; Taylor and Howard 2000; Wyns et al. 2004, Dewandel et al. 2006), on their hydrodynamic properties (Howard et al. 1992; Chilton and Foster 1995; Maréchal et al. 2004), on the development of methodologies for successful borehole siting (Barker et al. 1992), and, more recently, on methodologies for aquifer mapping and groundwater management at watershed scale (Lachassagne et al. 2001; Maréchal et al. 2006; Courtois et al. 2010; Dewandel et al. 2010).

The objective of this study is to assess the role of geological heterogeneities (dykes, fractures) and recharge dynamics on groundwater flow in a human-impacted sub-watershed based on detailed spatio-temporal field obser-

J. Perrin (✉)
BRGM, Water Division, Resource Assessment,
Discontinuous Aquifers Unit,
Indo-French Centre for Groundwater Research,
Uppal Road, 500 606 Hyderabad, India
e-mail: je.perrin@brgm.fr

S. Ahmed
National Geophysical Research Institute,
Indo-French Centre for Groundwater Research,
Uppal Road, 500 606 Hyderabad, India

D. Hunkeler
Centre of Hydrogeology and Geothermics (CHYN),
University of Neuchâtel,
Rue Emile Argand 11, 2009 Neuchâtel, Switzerland

variations. The study takes advantage of the very dense groundwater observation network constituted by irrigation wells. Such an approach complements experimental studies on heterogeneities at the experimental site scale such as borehole tests to assess connectivity and hydraulic properties of fractures (e.g., Paillet et al. 1987; Silliman and Robinson 1989; Paillet 1993; Paillet 2000; Day-Lewis et al. 2000, 2003; Le Borgne et al. 2006) and studies at large scale consisting of the mapping of lineaments for the location of groundwater potential zones using satellite imagery (e.g., Henriksen and Braathen 2006; Krishnamurthy et al. 1996; Sander et al. 1997; Sander 2007). It is believed that the observed field conditions are representative of the overall context of southern India; therefore, the conclusions of this work may be applicable elsewhere.

Local context and methods

The studied sub-watershed encompasses the village of Sangapur (17.82°N latitude, 78.66°E longitude) located 60 km north-east of Hyderabad, Andhra Pradesh, India (Fig. 1). The total sub-watershed area is 256 ha of which 53% (136 ha) is occupied by forest (eucalyptus plantation mainly). The remaining is occupied by farmland, fallow land, and the village. The main irrigated crops are rice and vegetables. Paddy area increases from 7.5 ha in the dry season to 13.5 ha during the monsoon season (two harvests per year), whereas vegetables cover 5.7 ha during dry season and 5.1 ha during monsoon. The main rainfed crops are cotton and maize.

The geology of the sub-watershed is composed of orthogneissic Archean granite typical of the entire region. The weathering profile was established from observations

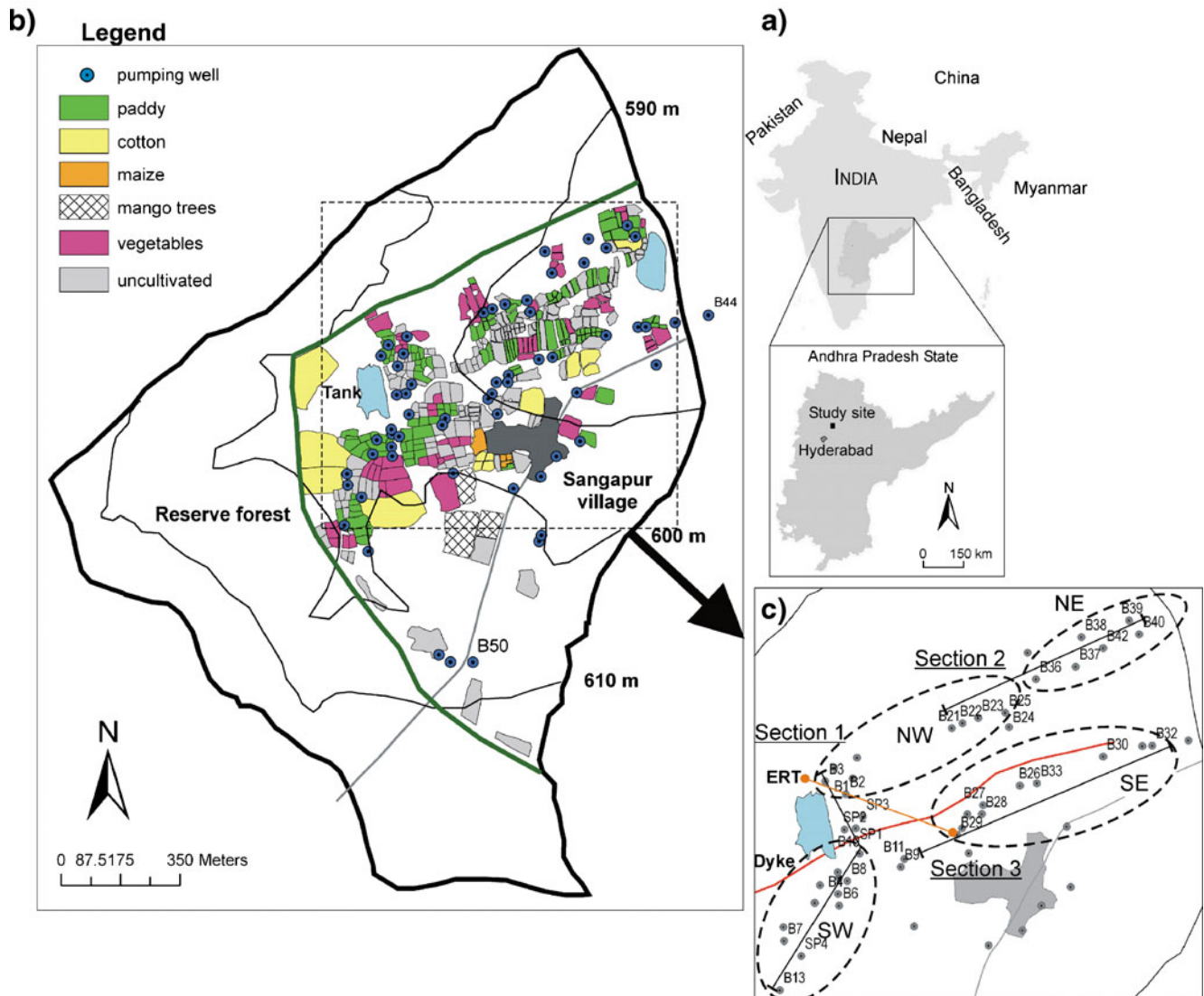


Fig. 1 a Location of the study area in the State of Andhra Pradesh, southern India. b The study area. Dry season land use of the studied watershed (bounded by the *thick black line*): uncultivated plots are cultivated during the rainy season; the limit with the reserve forest to the west and north is marked by the *thick green line*. Topographic elevation contours (m amsl) and boreholes (*blue points*) are also indicated. The zoom *c* shows the location of all the monitoring features (wells, etc.), sections and areas described in the text

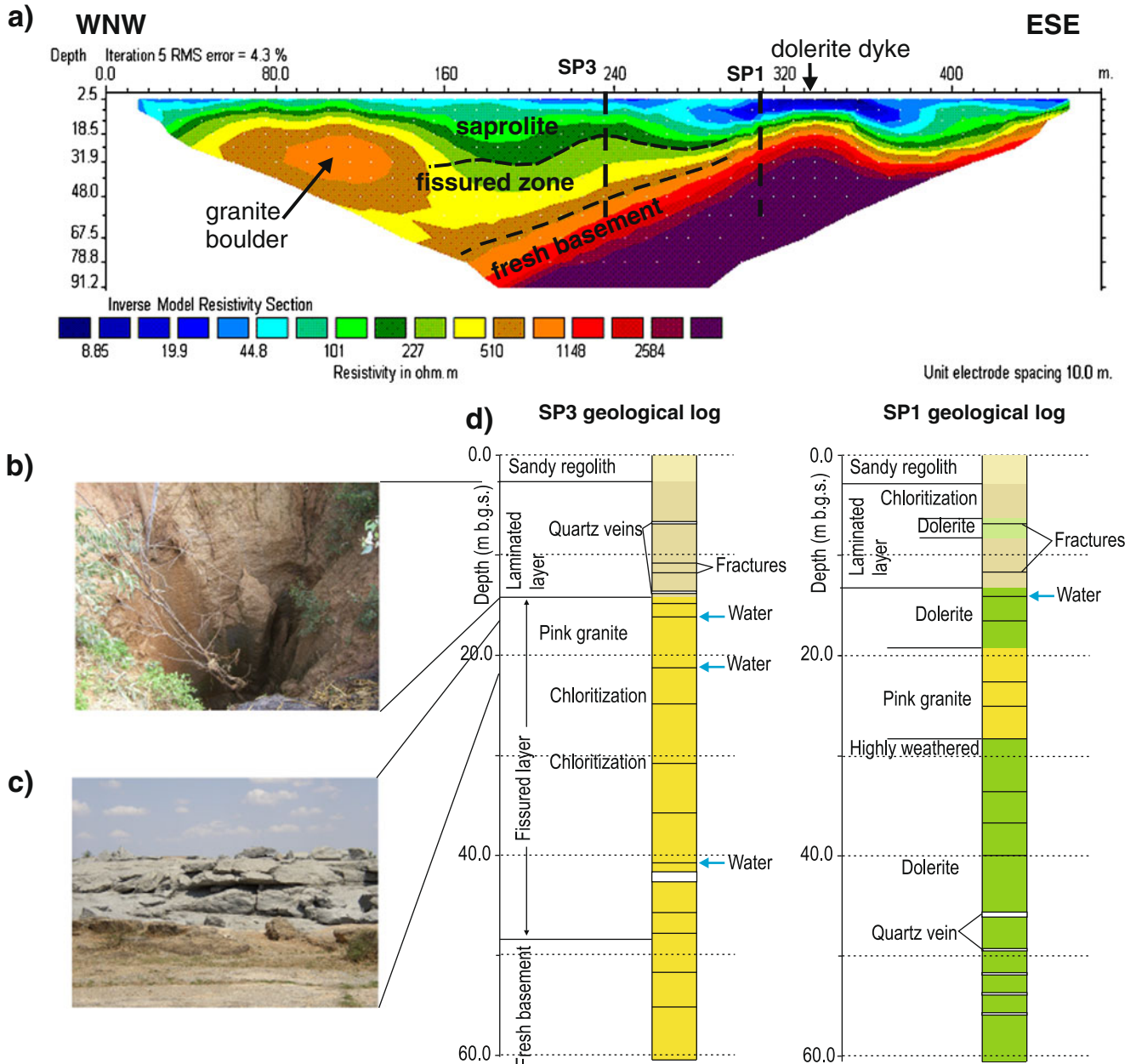


Fig. 2 a Electrical resistivity tomography (ERT) section along the trace shown in Fig. 1 indicating the presence of the dolerite dyke and a granite boulder within the granite weathered profile; b A view of the laminated layer in a defunct dug well; c The exposed fissured layer in a quarry a few kilometers west of the study site; d Geological logs of piezometers SP1 and SP3 from cuttings observations; their projected locations are also reported on the ERT section

in defunct dug wells, drilling of three piezometers, and resistivity tomography profiles. The weathering profile is very similar to other watersheds of the region (Dewandel

et al. 2006) with 0–2 m of sandy regolith, 10–15 m of laminated layer, and 25–40 m of fissured zone (Fig. 2). A dolerite dyke has intruded the granite (Figs. 1 and 2); it

Table 1 Groundwater budgeting at the sub-watershed scale. R is recharge, IRF irrigation return flows, PG groundwater pumping, E evaporation from the water table, Q_{out} groundwater flow at the downgradient limit of the watershed. Tank recharge ($Tank R$) corresponds to percolation from tank during the dry season. Tank percolation during the wet season is included in the general recharge term R . All the budget components are expressed in mm

	Rainfall	R	IRF	Tank R	PG	E	Q_{out}	Balance
March–July 2008	171	49.7	27.1	4.1	74.7	0.6	0.7	5.0
July 2008–June 2009	731	87.8	99.9	25.2	224.9	4.4	1.9	–27.2

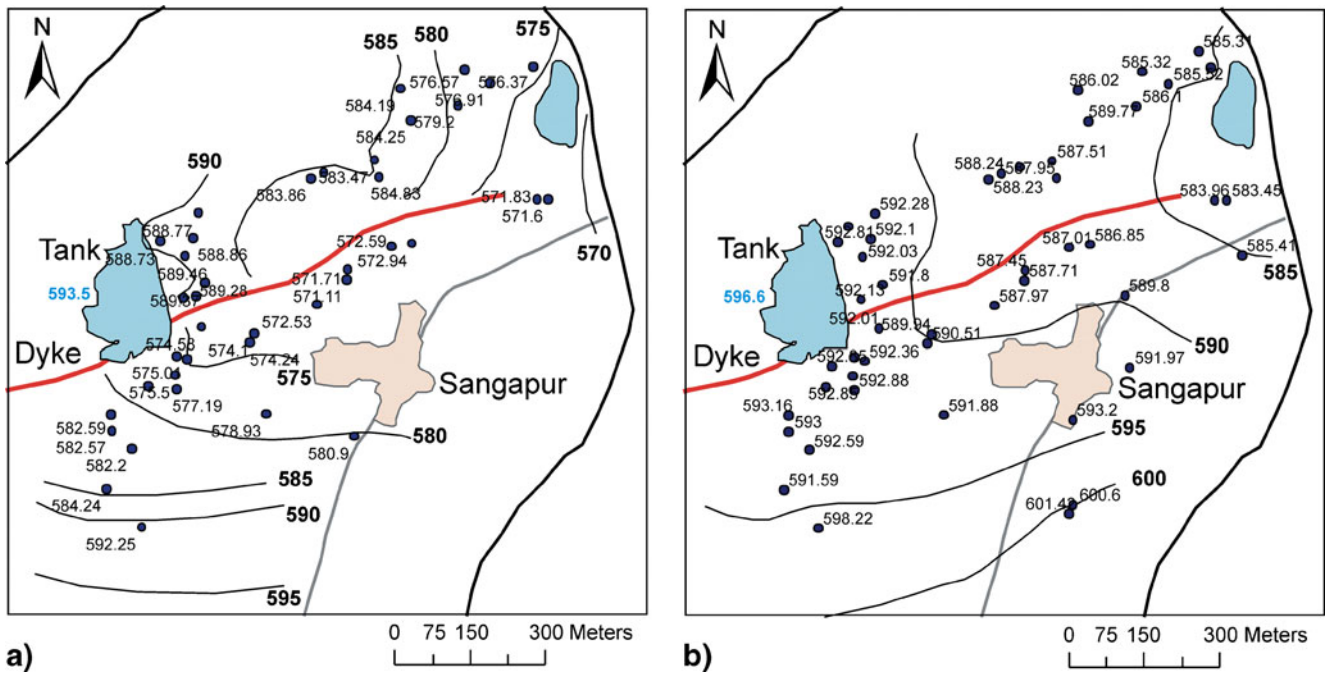


Fig. 3 a) Dry season piezometric map (39 observation points, 10 July 2008) and b) monsoon season piezometric map (50 observation points, 1 Oct 2008). The tank (earth dam) water-level elevation is indicated in blue. Elevation contours and observation point measurements are given in m amsl

extends beyond the extreme W of the sub-watershed and cuts through the study area to terminate near the NE corner of the sub-watershed (exact termination unknown). Its typical width is on the order of 40–50 m based on field observations and resistivity tomog-

raphy profiles. According to geophysical profiles and drill-cutting observations, the dolerite dyke is only weathered in the first 6–8 m below ground surface in agreement with a previous study on another dyke by Chandra et al. (2006).

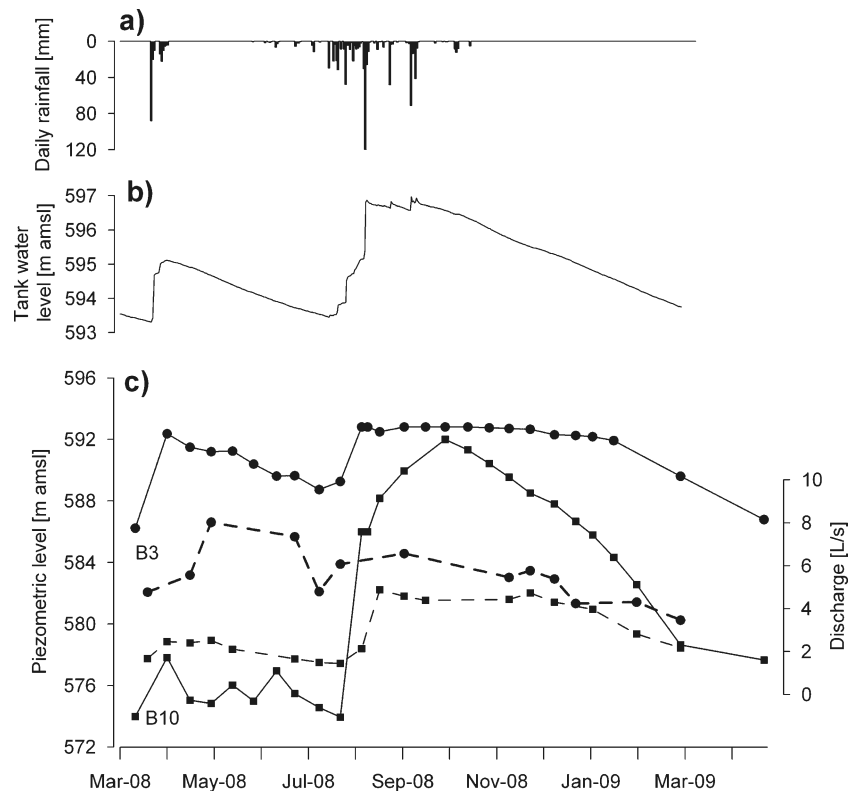


Fig. 4 a) Daily rainfall monitored in the sub-watershed; b) tank water-level variations; c) temporal variations of hydraulic heads (solid lines) and discharge (dashed lines) for representative wells B10 (south of dyke, squares) and B3 (north of dyke, dots)

Table 2 Observed static water levels in individual wells illustrating the water table rise caused by the monsoon recharge 2008

Well	10-Jul-2008 WL [m b.g.s.]	24-Jul-2008 WL [m b.g.s.]	7-Aug-2008 WL [m b.g.s.]	19-Aug-2008 WL [m b.g.s.]
B1	3.70	3.65	0.45	0.41
B10	19.10	19.72	7.68	5.51
B11	21.52	22.35	15.87	12.69
B12	13.21	13.00	NA	7.08
B13	13.90	14.15	12.31	NA
B14	4.61	3.53	1.02	1.03
B16	21.75	22.34	21.88	18.62
B17	18.21	18.39	NA	6.45
B18	6.55	1.15	0.40	0.60
B2	2.60	1.84	0.00	0.01
B21	6.99	6.93	NA	1.35
B22	6.72	6.41	NA	1.12
B24	3.27	1.90	NA	0.00
B25	5.51	4.36	NA	0.40
B26	17.99	18.82	NA	8.20
B27	19.78	20.32	9.32	9.47
B28	21.07	18.67	9.58	10.21
B29	20.95	21.92	15.89	12.56
B3	3.88	3.35	-0.20	0.12
B31	15.19	15.16	NA	5.95
B32	15.37	15.35	NA	6.42
B33	17.03	17.92	NA	7.06
B35	5.71	6.96	NA	3.21
B36	7.11	9.28	NA	1.07
B37	7.80	6.15	NA	0.65
B38	11.69	11.42	NA	3.89
B4	20.52	21.08	NA	7.10
B40	10.65	8.62	NA	1.68
B42	10.37	9.53	NA	2.43
B7	14.12	14.09	10.92	8.33
B8	21.23	21.84	12.46	10.75
B9	21.69	22.56	15.37	11.45
SP2	4.16	3.32	0.39	0.48
SP4	15.12	15.18	12.80	10.28

Historically, water during the 8-month long dry season was provided to the village by a small tank (earth dam) and, later during the twentieth century, shallow groundwater was exploited by 12 dug wells for small-scale irrigation. Presently, groundwater is intensively exploited by 39 irrigation wells (2 new wells drilled during the study period 2007–2009), eight wells for domestic use (including one municipal well for drinking supply) and poultry farms. These wells have an average depth of 60 m (range between 40 and 90 m) and have been mostly drilled since the 1990s. In addition, eight abandoned wells and three piezometers (drilled for the study) were used for piezometric measurements and hydraulic testing.

This large abstraction resulted in the over-exploitation of the resource with drying up of dug wells that can no longer be used and occurrence of intermittent discharge for some irrigation wells (three wells intermittent at all times, eight wells becoming intermittent during the dry season).

Groundwater budgeting at the sub-watershed scale was computed following the methodology of Maréchal et al. (2006): irrigation return flows (IRF), groundwater pumping (PG), evaporation from the water table (E), groundwater flow at the downgradient limit of the watershed (Q_{out}), and dry season recharge seeping from the tank (Tank R) are estimated from field surveys for both the dry and the wet seasons. The change in groundwater storage (ΔS) is given by the aquifer specific yield (S_y) multiplied by the observed water-table fluctuation during the selected period (Δh). Since the recharge (R) is not easily estimated, the groundwater balance is computed first for the dry season period when R is nil, this gives an estimate of S_y , all the other terms being computed from field surveys. Then, the

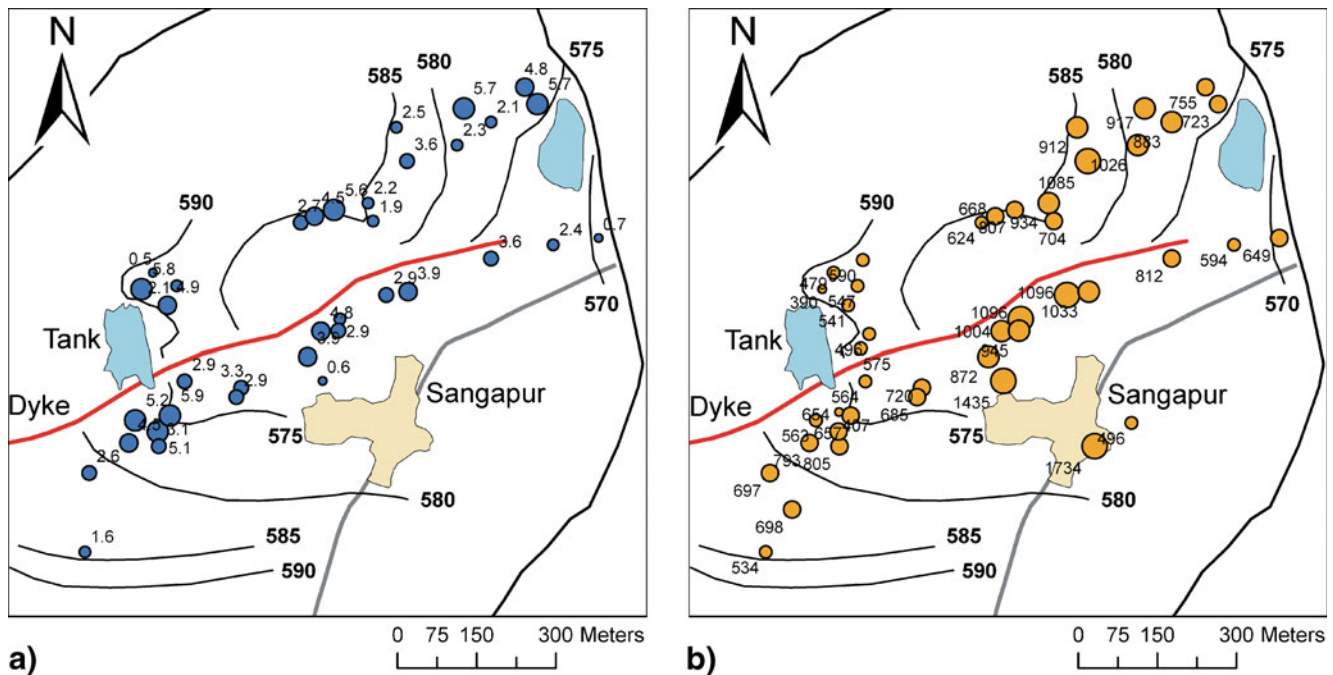


Fig. 5 a Well discharge map (in L/s) and b electrical conductivity map (in $\mu\text{S}/\text{cm}$) based on average values measured over a span of 1 year (March 2008–March 2009). The dot's size is proportional to the discharge/electrical conductivity value of each well. Dry season equipotentials are also shown (m amsl)

groundwater balance is computed for the wet season period using the specific yield obtained in the first step, leading to a representative estimation of the recharge term.

The groundwater balance shows a strongly negative groundwater balance even after the good monsoon rainfall of 2008 (Table 1). Computed specific yield from the water-table fluctuation and groundwater budget are 0.012 for the first recession (April to July 2008) and 0.0083 for the second recession (October 2008 to June 2009) following two rainy periods, within the same range as other values obtained in similar context (Maréchal et al. 2006; Dewandel et al. 2010).

The hydraulic conductivity of the dyke has been estimated by a pumping test in piezometer SP2 which partly intersects the dyke; analyzing the SP2 recovery with the Theis method gives 2.6×10^{-7} m/s. Hydraulic conductivity near the dyke is $2.3\text{--}2.5 \times 10^{-6}$ m/s, about one order of magnitude higher (tested by pumping SP2 and monitoring drawdown in SP1, and vice-versa). The aquifer hydraulic conductivity away from the dyke is about 2×10^{-5} m/s (pumping B2, monitoring SP3), which is two orders of magnitude higher than the dyke.

Field work was carried out on a fortnight basis from March 2008 to March 2009 with two additional campaigns in April and June 2009. Each time the piezometry was measured on 30–41 pumping wells, 6 abandoned wells, and 3 piezometers (since 10 July 2008) before the onset of pumping. These measurements correspond to pseudo-static groundwater level as last pumping typically ended about 8 h before piezometric measurements were taken. Then, after pumps were switched on (the government provides free power for pumping on a 7 h daily basis), the discharge and electrical conductivity (EC) of 18–28 irrigation wells were measured with a 20-L bucket and stopwatch (average of 3–5 measurements) and a WTW EC-meter 340i.

For the interpretation of wells showing increase in discharge and head during monsoon recharge, it is hypothesized that additional inflows occur within the newly saturated section of the aquifer in addition to the already existing steady-state inflow in the permanently saturated section.

In addition to these regular field surveys, two hydrochemical sampling campaigns were carried out, in October 2008 (end of the monsoon) and June 2009 (end of the dry season). During these surveys, 22 and 20 irrigation wells, respectively, and the percolation tank water were sampled for cations (100 ml, with acidification with HNO_3 65% suprapur) and anions (100 ml). Water temperature, EC, and pH were measured on site; bicarbonates were determined by titration in the laboratory within 48 h after sampling. Major ions were analyzed with a Dionex DX-120 ion chromatograph and quality of analysis was checked with ionic balance (all samples within 10%). In the framework of another study on the tank, daily rainfall had been measured with an automatic rain gauge located near the tank as well as tank water level with an automatic water level recorder (Perrin et al. 2009).

Results

Hydraulic heads

The general piezometric surface follows the topography and quite strong horizontal hydraulic gradients are observed (4% dry season, 1–2% monsoon) as expected from hard-rock aquifers with limited permeability (Fig. 3). The role of the dyke as an impermeable barrier to flow is clear during the dry season as it creates a well-marked hydraulic disconnection of the aquifer with a head drop of 5–15 m across the dyke. It seems that the dyke plays a clear role of barrier in the eastern part of the study area as a head drop can be inferred even if the dyke could not be mapped.

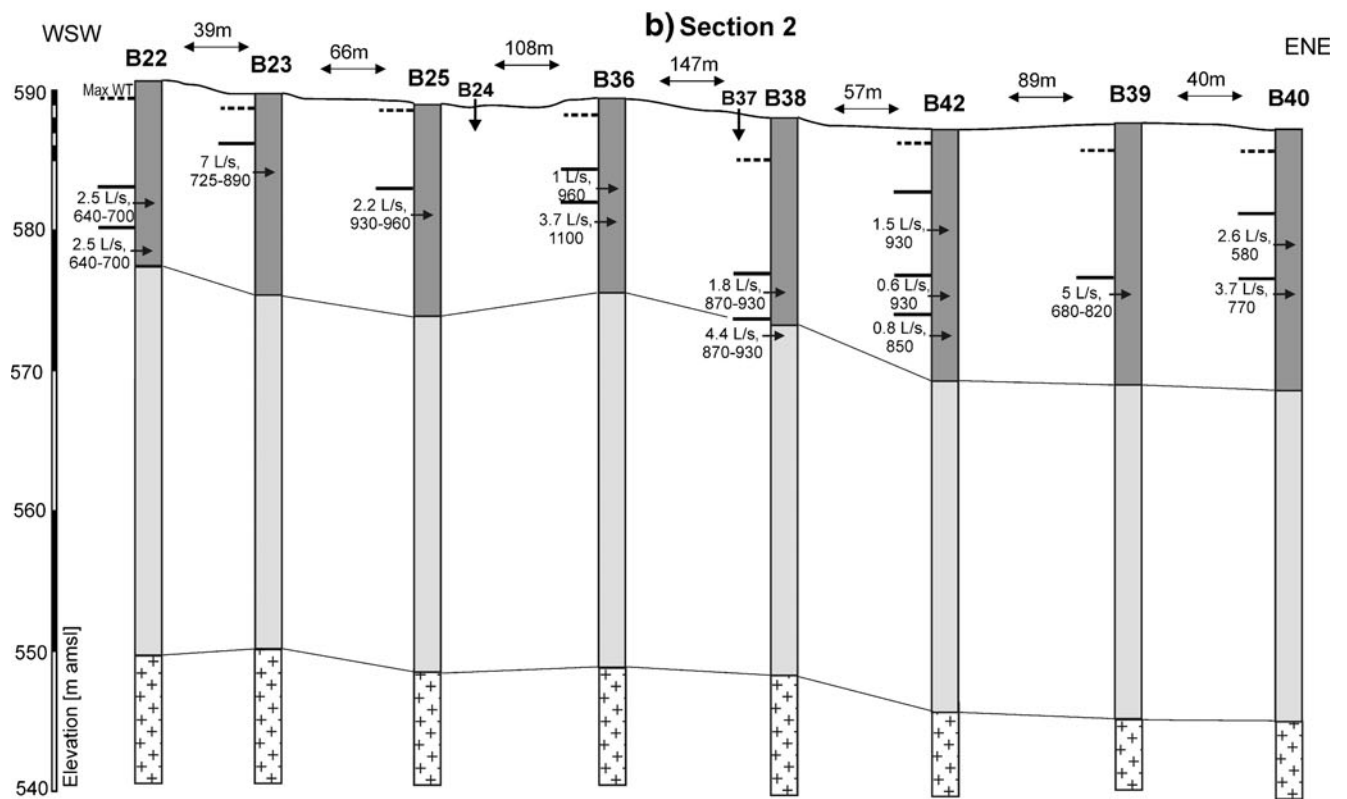
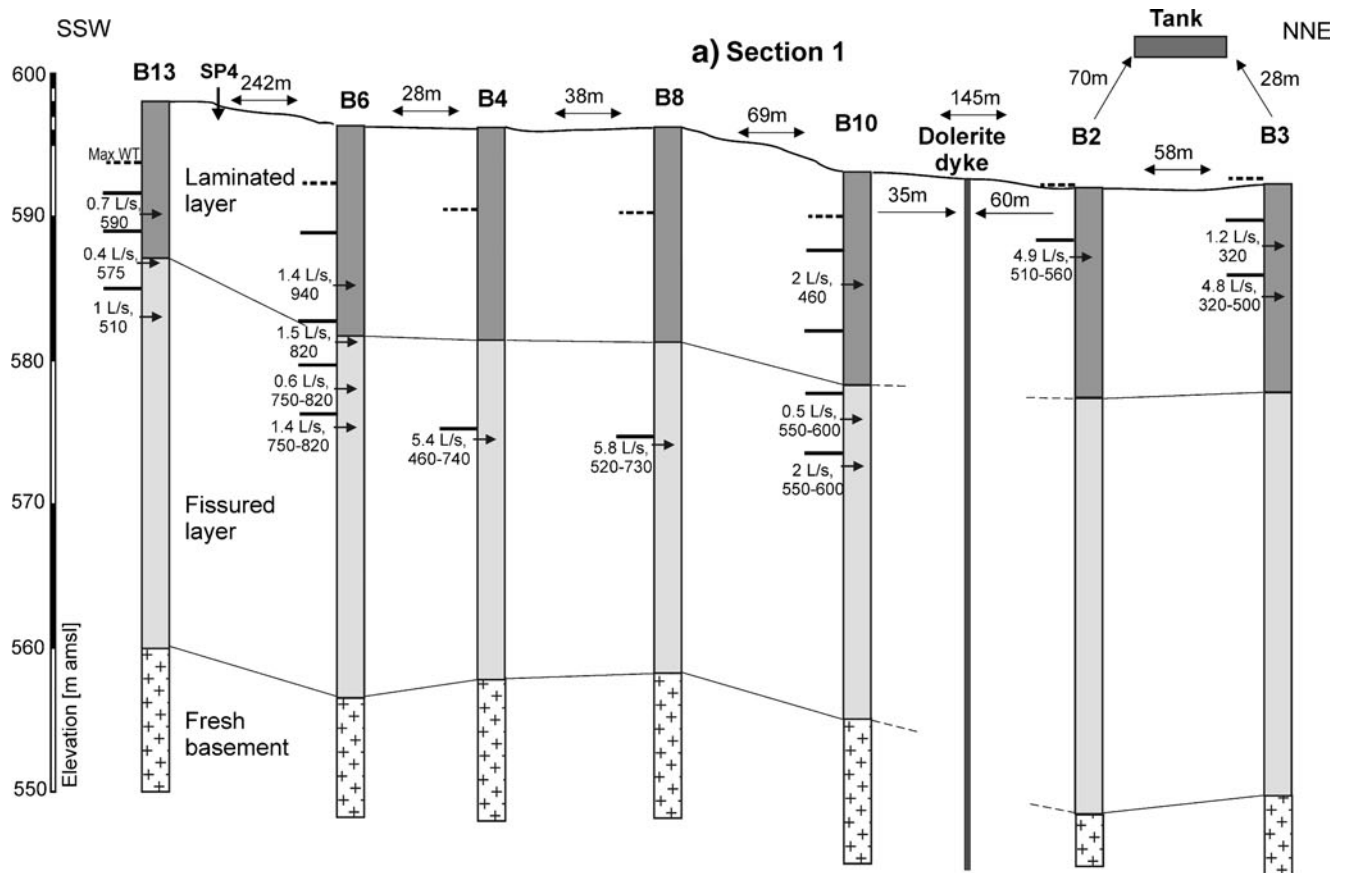
During the monsoon season, the general rise of the water-table connects again the two parts of the aquifer. This connection occurs within a few weeks as shown by the observed rapid rise in hydraulic heads for two representative piezometers, one on each side of the dyke (Fig. 4). During the monsoon 2008, all monitored wells show an increase in hydraulic head after the first large rainfall events, occurring between 16–27 July (172 mm, Fig. 4); heads start increasing between 16–23 July for some of the wells and 25 July–6 August for the rest of the wells (Table 2). This indicates rapid transit of recharge water through the unsaturated saprolite. Additional rainfall events occur on 9 August (120 mm), 25 August (48 mm) and 8–11 September (130 mm), and highest recorded heads in monitored wells typically occurred by end of September.

Well discharges

High spatial variability in well discharge is observed with no evident spatial correlation (Fig. 5). Average discharge is 3.3 L/s (12 m³/h), minimum discharge 1.6 L/s (5.7 m³/h, well B13), and maximum discharge 5.9 L/s (21 m³/h, well B8). Modest discharge and high spatial variability is expected in crystalline aquifers where most well productivity is provided by the heterogeneous fissured network.

Temporal discharge variations are evident for the majority of wells, with a discharge decrease during the dry season (Fig. 6). Out of 28 wells for which both hydraulic head and discharge time series are available, 15 show a clear decrease in discharge during periods of lower water table: 4 wells located to the north of the dyke (29%

Fig 6 Cross-sections of the studied aquifer (locations on Fig. 1): **a** section 1, **b** section 2, **c** section 3. Geological contacts are estimated from geophysical data (ERT and resistivity logging in three abandoned wells) and piezometer drilling (between B2 and B10). Water level, and discharge and EC data (every two weeks from March 2008 to March 2009, given in L/s and $\mu\text{S}/\text{cm}$, respectively) are used to determine the location of inflows in the wells and the EC value of the inflows. On the left side of each well log, *dashed lines* indicate observed maximum water levels and *solid lines* represent measured static groundwater levels below which clear decrease in discharge has been observed. This is used to infer the successive locations of hydraulically active fracture zones with their respective yield (given by the difference between the well discharge measured when the static water table is respectively above and below the *solid line elevation*) and EC



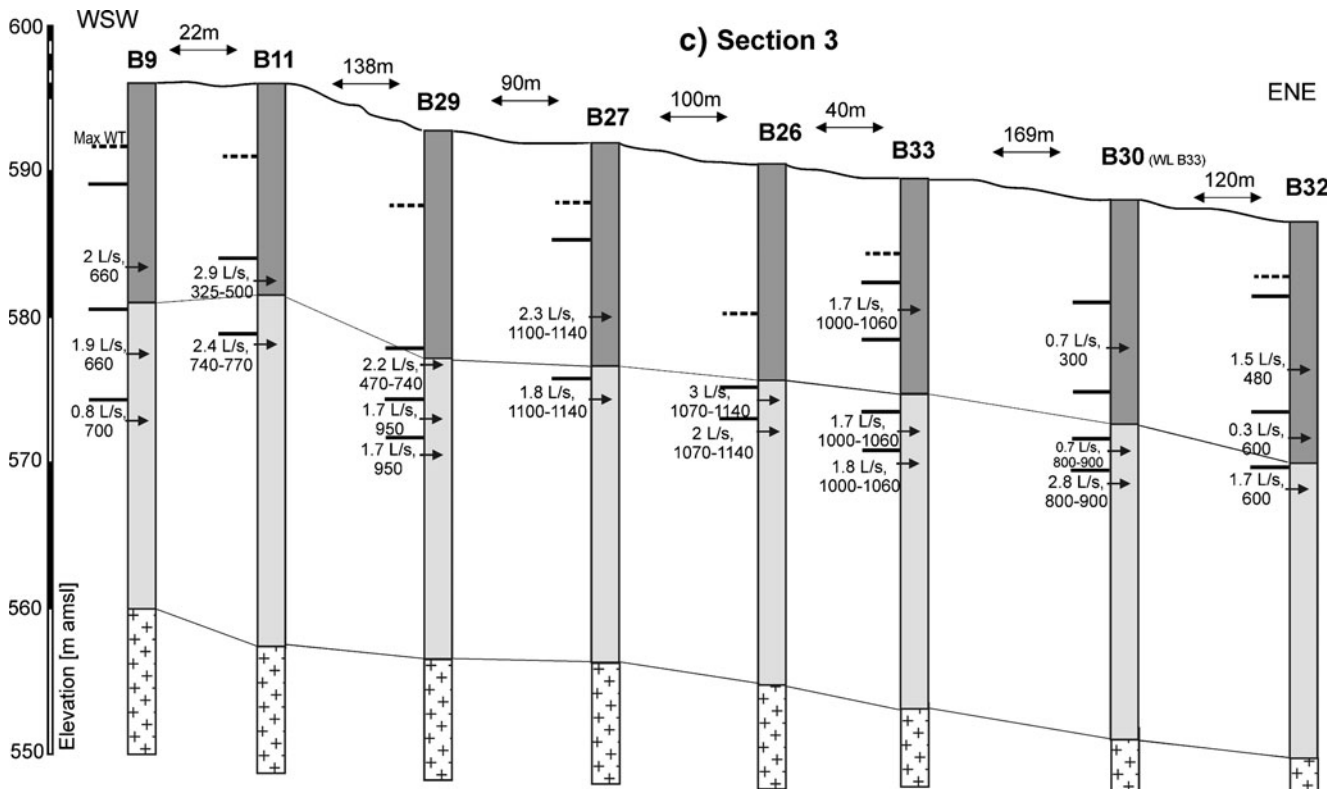


Fig. 6 (continued)

of the monitored wells in this aquifer compartment), 11 wells located to the south of the dyke (79% of the monitored wells in this aquifer compartment). The remaining 13 wells show no clear correlation with the water table. The average discharge of these 15 wells drops from 5.1 to 1.6 L/s. Discharge decrease occurs when the static water table before pumping is located below 8–10 m b.g.s (Fig. 7). For the water-table range of 8–15 m b.g.s, the pump rate diminishes by 0.4 L/s for each meter of decrease in the static water level before pumping (17 observations), whereas below 15 m, the pumping rate diminishes by 1.1 L/s. It should also be noted that, for two wells, no change in discharge is noted even if the water table reaches levels below 21 m b.g.s. (Fig. 6a, wells B4 and B8 which are near each other and may be fed by a deeper fracture zone).

For all the wells located just south of the dyke (B10, B12, B27, B28, B32, B33), discharge decrease during depletion first occurs when the water table drops below 5–9 m b.g.s. (average 7.2 m), which is consistent with the role of hydraulic discontinuity played by the dyke below this reported depth.

Variations in well discharge may be caused by a decrease in aquifer transmissivity as the water table gets lower and as a consequence of the pump characteristics, with a decreasing pump rate as the water has to be lifted over a larger height. All the irrigation wells are equipped with similar three-phases 5 HP submersible pumpsets (3.73 kW). With a 5 HP submersible pump having an efficiency higher than 30% as indicated by manufacturers (brands Texmo and Crompton-Greaves are most in use),

potential delivered flow is at least 4.6 L/s for a total head of 25 m (Fraenkel 1986), that is higher than most measured flow rates in the field. Moreover, pumps are either on or off depending on power availability and no valves are set for discharge regulations. Therefore observed pumping rate decrease is primarily due to a decrease in aquifer transmissivity and as a consequence pumps produce lower yields. This is illustrated by the widespread intermittence observed when hydraulic heads drops during the dry season (pumps are running but aquifer transmissivity is not sufficient to deliver a

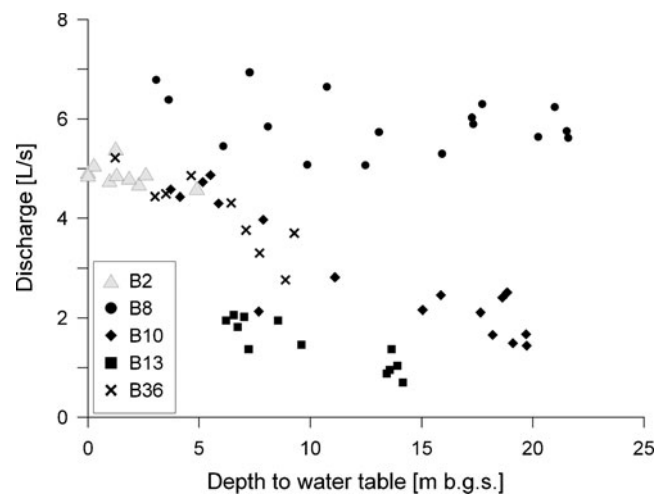


Fig. 7 Evolution of discharge as a function of static piezometric level (recorded before pumping) for five representative irrigation wells

Table 3 Basic statistics of hydrochemical parameters measured in the four aquifer compartments for two sampling campaigns (October 2008 and June 2009). EC in $\mu\text{S/cm}$, T in $^{\circ}\text{C}$, all the other parameters in mg/L

		EC	pH	T	Ca	Mg	Na	K	Cl	SO ₄	NO ₃	F	HCO ₃
October 2008 (end of monsoon)													
NW	Mean	583	NA	NA	76.4	20.5	38.0	0.7	22.3	31.9	12.5	1.0	343
	Min	279	NA	NA	40.6	6.2	15.9	0.4	4.9	6.6	2.2	0.6	176
	Max	750	NA	NA	93.1	29.9	55.1	1.1	37.1	53.5	29.7	1.4	424
NE	Mean	847	NA	NA	95.6	635.3	56.9	1.4	64.1	52.8	28.4	1.5	410
	Min	715	NA	NA	69.5	34.8	46.7	0.8	41.3	43.7	7.5	0.6	376
	Max	1,063	NA	NA	135.7	48.4	62.1	2.0	82.5	69.4	42.6	1.8	543
SW	Mean	475	NA	NA	60.0	13.7	36.8	0.6	11.2	16.4	16.0	1.5	289
	Min	315	NA	NA	37.3	6.6	26.0	0.4	6.5	8.4	1.7	0.8	173
	Max	661	NA	NA	89.2	21.2	52.0	0.9	18.1	26.5	48.4	2.3	408
SE	Mean	751	NA	NA	96.8	23.4	60.1	1.0	58.4	40.5	35.3	1.9	380
	Min	497	NA	NA	57.5	14.4	38.9	0.4	29.0	22.0	8.8	1.4	259
	Max	1,032	NA	NA	125.3	33.8	76.8	2.4	90.0	60.3	63.3	2.3	453
June 2009 (end of dry season)													
NW	Mean	634	7.2	30.5	71.1	19.7	36.2	0.6	25.5	28.9	14.9	1.5	350
	Min	384	7.0	30.1	52.0	6.9	16.5	0.4	7.1	9.2	3.6	0.6	231
	Max	960	7.2	30.9	83.4	38.3	67.2	1.0	81.2	56.6	10.0	1.9	449
NE	Mean	941	7.1	30.5	83.8	36.1	54.6	0.8	69.8	66.7	22.6	1.6	428
	Min	840	7.0	30.0	62.8	32.2	50.2	0.7	60.7	56.3	6.1	0.9	397
	Max	1,062	7.2	31.0	104.2	38.1	62.0	0.9	81.9	77.8	32.4	2.5	473
SW	Mean	557	7.0	30.4	59.0	15.8	35.3	0.6	13.8	20.4	20.4	1.6	325
	Min	302	6.7	30.0	29.1	5.5	24.2	0.4	7.5	7.2	7.4	0.0	154
	Max	671	7.4	31.0	77.3	23.6	46.8	1.0	18.2	31.2	51.6	2.7	414
SE	Mean	865	7.0	30.7	86.0	23.8	56.3	1.2	67.9	46.5	28.6	2.2	380
	Min	602	6.9	29.8	62.3	15.2	38.9	0.3	37.3	29.4	14.4	1.6	296
	Max	1,053	7.1	31.6	102.2	26.2	69.9	2.9	101.6	60.2	64.9	3.0	420

sustained constant yield) and also in the case of the presence of deep high-transmissivity fractures (e.g., wells B4 and B8), seasonal water-table fluctuations do not impact the well yields (if pumps were of lower capacity, a decrease in discharge would be expected).

Groundwater chemistry

Two sets of data have been collected to assess groundwater chemistry spatial and temporal variability: electrical conductivity (EC) of pumping wells on a fortnight basis during 1 year and two sampling campaigns for major ions on pumping wells and the water tank. Data show an extreme spatial variability in groundwater chemistry as illustrated by the average EC map (Fig. 5b). Two zones of higher mineralization can be identified, one near the village and the other in the northern part of the study area; groundwater points in the vicinity of the tank have a lower mineralization.

Two sampling campaigns were carried out, one at the end of the monsoon in October 2008 and one at the end of the dry season in June 2009. Results for major ions show that groundwater is of Ca–Mg–(Na)–HCO₃ type. Samples were classified in four groups (NW, NE, SW, SE) based on their location relative to the dyke (i.e., north or south) and based on their position upgradient or downgradient of the tank/village (i.e., west or east; Fig. 1). Groups to the west (NW and SW) present typically lower major ion concentrations (Table 3; Fig. 5b). Higher concentrations in the downgradient sector of the aquifer cannot be attributed to progressive mineralization along flowpaths because the most down-

gradient wells (B32, B40) are less mineralized. Attribution is given to sources of higher mineralization around B26–B27–B33 (likely impact of village sewage and poultry farms) and to B36 (likely impact of dumping site in a defunct dug well; Fig. 5b). The chemical specificities of the four groups seem not significantly influenced by the monsoon recharge as shown by concentrations observed in October 2008 and June 2009 (Table 3), indicating limited water exchange between the different zones of the aquifer. Scatter plots of representative ions (Na, Cl, SO₄) reveal different behaviors for the four groups: on SO₄–Cl plots, NW and SW group wells are aligned along a single correlation line, whereas the NE and the SE wells follow separate correlation trends. In contrast, on Cl–Na plots, NW and SW wells lay on separate correlation lines, whereas NE and SE follow they same trend. Well B24 shifts from its original NW group in October 2008 to the SE group in June 2009 (Fig. 8). The observed correlations between conservative ions is indicative of mixing of lower and higher concentration zones within each group, in other words samples plot along mixing lines.

Groundwater chemistry temporal variations as indicated by EC measurements can be subdivided into two periods: the dry seasons (April–June 2008, December 2008–March 2009) where either stable concentrations or a progressive increase in concentrations occur for most observation points (Fig. 9), and the monsoon season (July–November 2008) where three patterns can be observed. In most cases dilution occurs due to less mineralized recharge water (and more especially near the tank), in some cases higher concentrations occurs in the

SW zone with observations at SP4, B13 and B6, and finally no changes are observed at wells B1, B25 (NW zone) and B27, B33 (SE zone; Figs. 6 and 9).

Discussion and conclusions

The detailed field study on a less than 1 km² area of aquifer exploited by a high density of pumping wells (>40) reveals very high spatial variability in terms of hydraulic parameters (discharge, transmissivity) and groundwater chemistry. This variability can be explained by geological factors and the impact of human activities: a dolerite dyke cuts across the study area from west to east and acts as an impermeable barrier to flow as already described in other studies (Babiker and Gudmundsson 2004; Chandra et al. 2006). After monsoon recharge, the two aquifer compartments separated by the dyke may become hydraulically connection temporarily as indicated by piezometric mapping (Fig. 3). Spatial variability in discharge is due to the high complexity of the fracture network which contributes the most to the aquifer transmissivity (e.g., Maréchal et al. 2004) and as a conse-

quence of well discharge; this is illustrated by the observed decrease in discharge for the majority of wells as the water table lowers and parts of the transmissive fractures get dewatered (Fig. 6). The clear decrease in well discharge when hydraulic heads drop within the lower part of the saprolite/top zone of the fissured layer seems to corroborate the aquifer model of Dewandel et al. (2006) which indicates that the top zone of the fissured zone is the most transmissive but that some discharge is also produced by preserved fissures in the saprolite.

The prominent role of geological discontinuities and the fracture network in controlling groundwater flow contribute to the compartmentalization of the aquifer system. This compartmentalization also becomes evident when considering the chemical constituents in the aquifer. The presence of well-defined mixing lines in scatter plots of ions indicates four main compartments within which mixing occurs.

The compartmentalization of geological origin is further enhanced by well pumping that has completely modified the natural flow field and created a situation of “hydraulic containment”. Moreover, groundwater chemistry is also significantly modified by human impacts on

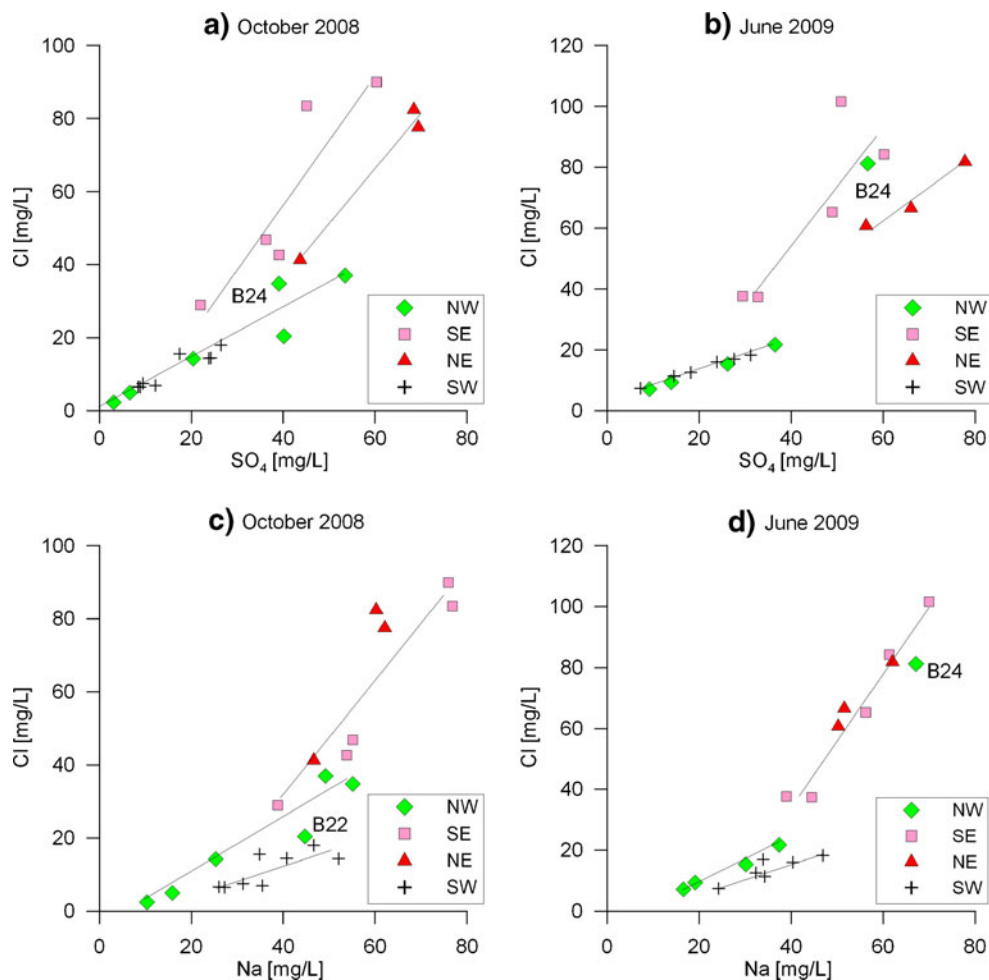


Fig. 8 Scatter plots of a–b SO₄–Cl and c–d Cl–Na showing the existence of mixing lines, characteristic of the four identified aquifer compartments (NW, NE, SW, SE)

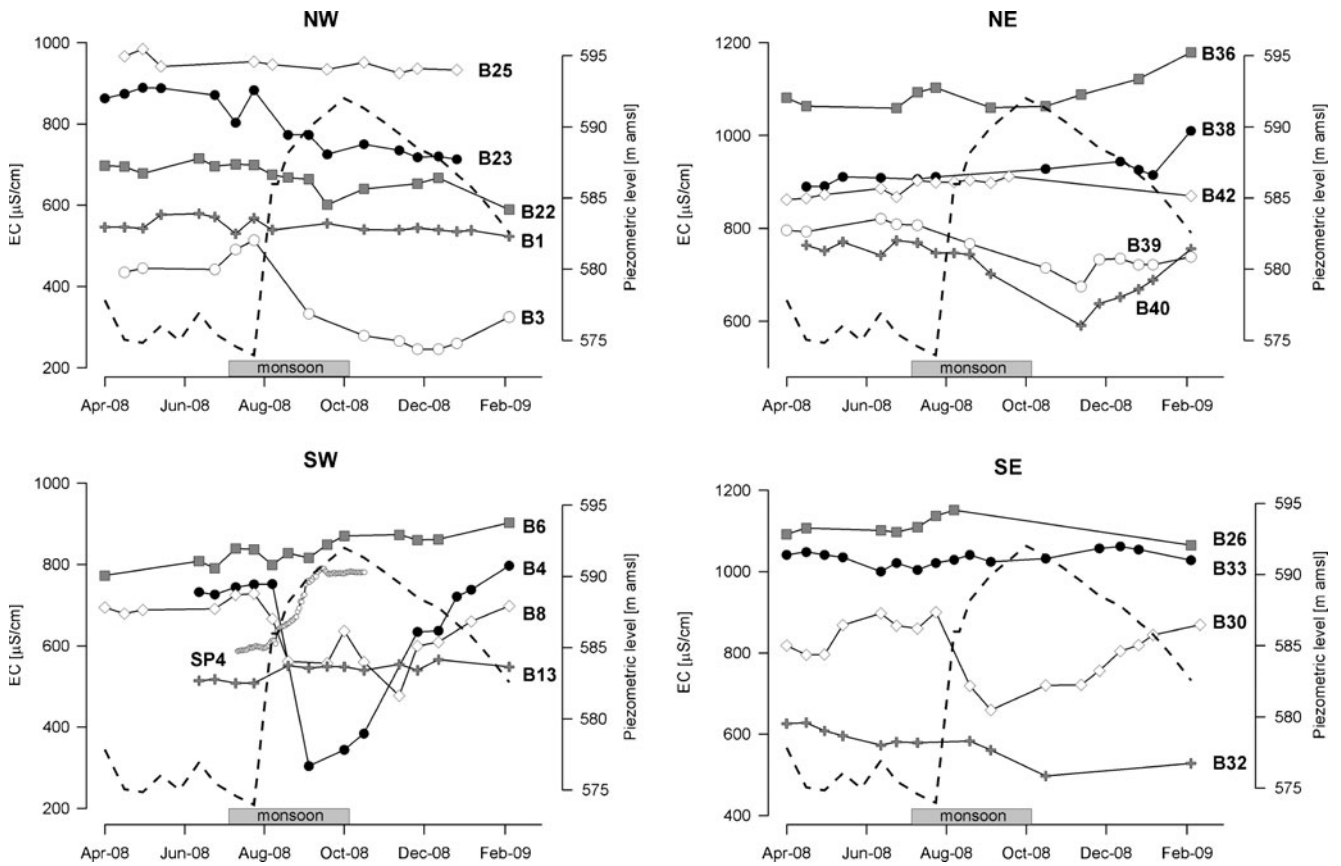


Fig. 9 Temporal evolution of EC in the four aquifer zones and representative piezometric levels (well B10, *dashed line*) to indicate when recharge occurs

aquifer recharge (irrigation return flows, tank percolation), solute recycling (Perrin et al. 2011) and additional chemical inputs (fertilizer, sewage).

Based on piezometric mapping alone, the aquifer seems to have continuity (with the exception of the dyke barrier during the dry season); however, groundwater

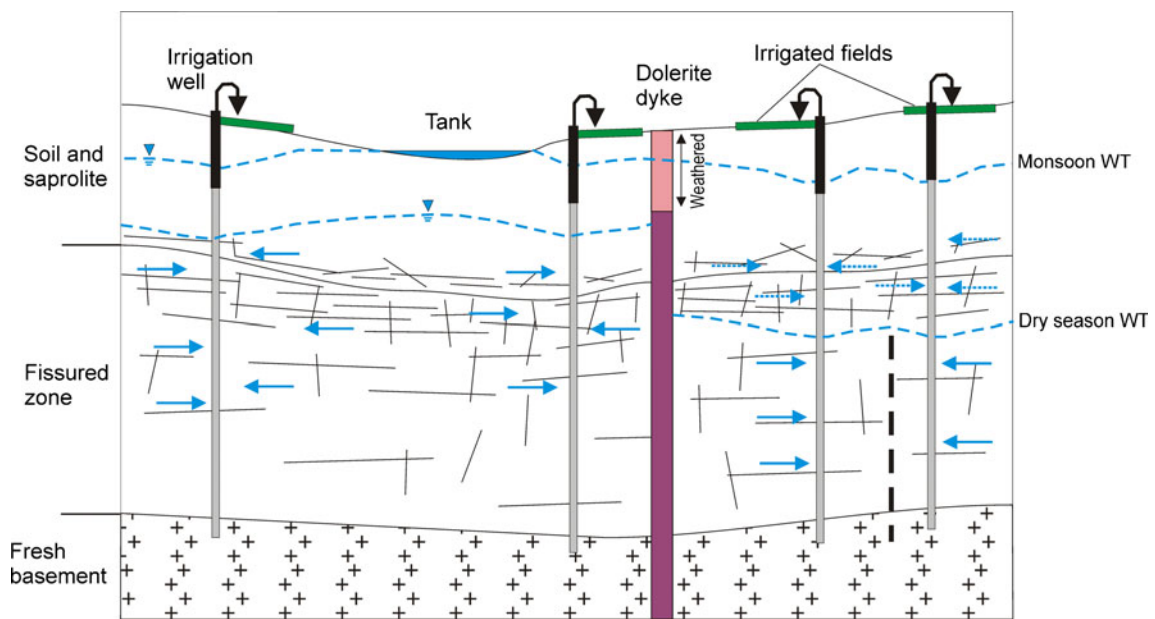


Fig. 10 Conceptual model of the aquifer dynamic functioning. *Blue solid arrows* indicate permanent flow, *blue dashed arrows* seasonal flow. The *dashed vertical line* indicates temporary aquifer compartmentalization caused by water-table decline. Wells' cased sections are in *black* and open well sections in *light grey*

chemistry shows that several compartments indeed exist and are characterized by their specific chemistry.

After significant rainfall, most monitoring wells show a quite rapid increase in hydraulic heads combined with a decrease in EC in many of them (Figs. 4, 6 and 9). This indicates that rapid recharge of less mineralized water takes place through the unsaturated saprolite. For wells near the tank, indirect recharge from tank water also contributes to the observed changes. On the other hand, for a few wells (B6, B13, SP4), hydraulic head increase is combined with an increase in EC.

The increase in EC may be explained by two different processes or a combination of both: (1) dissolution by recharge water of salts that were deposited in the topsoil during the dry season leading to highly mineralized recharge water; (2) a threshold effect such as two compartments of the aquifer, the upgradient one being more mineralized, which are disconnected below a given threshold corresponding to the elevation of the deepest connecting fracture and get connected as the water table rises above the threshold during recharge.

Wells B38 and B42 present a progressive trend towards higher EC with limited influence of recharge events; this trend may be attributed to the formation of a higher-mineralization plume, issued from the B36 area where a defunct dug well is used as a dumping site, that is progressively reaching downgradient areas.

To summarize the main processes identified from field data interpretation, a conceptual model of the aquifer functioning is proposed (Fig. 10). The two main layers of the aquifer are represented: the saprolite which is mostly unsaturated during the dry season and the fissured layer which provides most of the flow to the pumping wells. During the dry season when the water table gets depleted due to the absence of recharge and intensive pumping, the dolerite dyke acts as an efficient barrier to flow and splits the aquifer into two compartments when the water table gets below 6–8 m depth; as the water table gets deeper more disconnection may occur as illustrated on the right hand side of the diagram (dashed vertical line) because part of the fracture network gets dewatered. This process leads also to a clear drop in well discharges. This compartmentalization of the aquifer contributes to the spatial variability of groundwater chemistry which is enhanced by pumping and associated return flows.

During the monsoon season, after intense rainfall events, rapid piezometric rise is observed indicating that the aquifer behaves as an unconfined dynamic system, well discharge increases as a result of increased transmissivity and existing compartments get connected when piezometric levels rise above specific thresholds (e.g., 6–8 m b.g.s. in the case of the dyke, 10–17 m when the bottom of the saprolite is reached).

The consequences of this conceptual model is that hard-rock aquifers have to be described as transient unconfined aquifers with highly variable hydraulic heads, discharge (and transmissivity), and connectivity. The aquifer connectivity will vary according to hydraulic heads and therefore any numerical modeling of flow and

solute transport has to integrate this type of threshold (reservoir models may be more adapted than distributed models). Pumping well discharges can decrease significantly as a result of hydraulic head drop. This behavior is expected in unconfined aquifers (Rushton 2003, pp. 173 and 259) and may be dramatic if the high permeability zone is in the upper part of the aquifer that dewateres first, as is the case in hard-rock aquifers. This discharge variability has to be taken into consideration when assessing groundwater abstraction for groundwater balance computation, for instance (i.e., a single measurement of pumping rate may be very different from the annual average). The hydraulic role of the dyke as a barrier to flow may be used for groundwater management: protection, borehole siting, artificial recharge.

Using conservative natural tracers, it has been possible to distinguish four aquifer compartments within which groundwater mixing occurs. These compartments have a dimension of 400–500 m along the general groundwater flow direction. This scale may be representative of the connectivity of the fissured network. Intensive pumping (and over-exploitation) has enhanced the compartmentalization of the aquifer; therefore, if management measures recommend more limited abstraction rates, this may reconnect parts of the aquifer and in turn modify the groundwater quality of the downgradient compartments.

The presented conceptual model is likely to be representative of hard-rock aquifers of southern India which are intensively exploited, since the climatic, geological, and farming contexts are very similar over the entire region. The findings of this study corroborate earlier studies showing that in these aquifers most of the transmissive fractures occur in the top of the fractured zone (Briz-Kishore 1993; Dewandel et al. 2006), and drilling deep wells (>40–50 m) is not an option in case of failure because it can lead to unbearable economic consequences for farmers (Maréchal 2010).

There is a need for better information in farming communities on how these aquifers behave so as to limit over-exploitation, crop losses, and economic strains. Ideally, groundwater use should revert to a community-based management of the water resource. A field visit in June 2010 showed that within 1 year, nine new irrigation wells had been drilled in this already over-exploited aquifer.

Acknowledgements We are indebted to the students (J. Cachera, E. Bougon, M. Ahmad) who contributed to the collection of field data and to Mr Wajiduddin for his continuous involvement in field activities. The community of Sangapur is warmly thanked for its support and interest in this research project. We are grateful to the Editors and two anonymous reviewers for their valuable comments on the original manuscript.

References

- Acworth RI (1987) The development of crystalline basement aquifers in a tropical environment. *Q J Eng Geol* 20:265–272
- Babiker M, Gudmundsson A (2004) The effects of dykes and faults on groundwater flow in an arid land: the Red Sea Hills, Sudan. *J Hydrol* 297:256–273

- Barker RD, White CC, Houston JFT (1992) Borehole siting in an African accelerated drought relief project. *Geol Soc Spec Publ* 66:183–201
- Briz-Kishore BH (1993) Assessment of yield characteristics of granitic aquifers in South India. *Ground Water* 31(6):921–928
- Chandra S, Rao VA, Krishnamurthy NS, Dutta S, Ahmed S (2006) Integrated studies for characterization of lineaments used to locate groundwater potential zones in a hard rock region of Karnataka, India. *Hydrogeol J* 14:767–776
- Chilton PJ, Foster SSD (1995) Hydrogeological characterization and water-supply potential of basement aquifers in tropical Africa. *Hydrogeol J* 3(1):36–49
- Courtois N, Lachassagne P, Wyns R, Blanchin R, Bougäiré FD, Somé S, Tapsoba A (2010) Large-scale mapping of hard-rock aquifer properties applied to Burkina Faso. *Ground Water* 48(2):269–283. doi:10.1111/j.1745-6584.2009.00620.x
- Day-Lewis FD, Hsieh PA, Gorelick SM (2000) Identifying fracture-zone geometry using simulated annealing and hydraulic connection data. *Water Resour Res* 36(7):1707–1721
- Day-Lewis FD, Lane JW, Harris JM, Gorelick SM (2003) Time-lapse imaging of saline tracer transport in fractured rock using difference-attenuation radar tomography. *Water Resour Res* 39(10):1290. doi:10.1029/2002WR001722
- Dewandel B, Lachassagne P, Wyns R, Maréchal JC, Krishnamurthy NS (2006) A generalized 3-D geological and hydrogeological conceptual model of granite aquifers controlled by a single or multiple weathering. *J Hydrol* 330:260–284
- Dewandel B, Perrin J, Ahmed S et al (2010) Development of a tool for managing groundwater resources in semi-arid hard rock regions: application to a rural watershed in south India. *Hydrol Proc* 24(19):2784–2797
- Fraenkel PL (1986) Water lifting devices. *FAO Irrigation and Drainage Paper* 43, FAO, Rome
- Gustafson G, Krásný J (1994) Crystalline rock aquifers: their occurrence, use and importance. *Appl Hydrogeol* 2:64–75
- Henriksen H, Braathen A (2006) Effects of fracture lineaments and in-situ rock stresses on groundwater flow in hard rocks: a case study from Sunnfjord, western Norway. *Hydrogeol J* 14:444–461
- Howard KWF, Hughes M, Charlesworth DL, Ngobi G (1992) Hydrogeologic evaluation of fracture permeability in crystalline basement aquifers of Uganda. *Appl Hydrogeol* 1:55–65
- Jones MJ (1985) The weathered zone aquifers of the basement complex areas of Africa. *Q J Eng Geol Hydrogeol* 18:35–46
- Krishnamurthy J, Kumar NV, Jayaraman V, Manivel M (1996) An approach to demarcate ground water potential zones through remote sensing and geographical information system. *Int J Remote Sens* 17:1867–1884
- Lachassagne P, Wyns R, Bérard P, Bruel T, Chéry L, Coutand T, Desprats JF, Le Strat P (2001) Exploitation of high-yield in hard-rock aquifers: downscaling methodology combining GIS and multicriteria analysis to delineate field prospecting zones. *Ground Water* 39(4):568–581
- Le Borgne T, Bour O, Paillet FL, Caudal JP (2006) Assessment of preferential flow path connectivity and hydraulic properties at single-borehole and cross-borehole scales in a fractured aquifer. *J Hydrol* 328:347–359. doi:10.1016/j.jhydrol.2005.12.029
- Maréchal JC, Dewandel B, Subrahmanyam K (2004) Use of hydraulic tests at different scales to characterize fracture network properties in the weathered-fractured layer of a hard rock aquifer. *Water Resour Res* 40:W11508, 17 pp
- Maréchal JC, Dewandel B, Ahmed S, Galeazzi L, Zaidi FK (2006) Combined estimation of specific yield and natural recharge in semi-arid groundwater basin with irrigated agriculture. *J Hydrol* 329:281–293. doi:10.1016/j.jhydrol.2006.02.022
- Maréchal JC (2010) Editor's message: the sunk cost fallacy of deep drilling. *Hydrogeol J* 18:287–289
- Paillet FL, Hess AE, Cheng CH, Hardin E (1987) Characterization of fracture permeability with high-resolution vertical flow measurements during borehole pumping. *Ground Water* 25(1):28–40
- Paillet FL (1993) Using borehole geophysics and cross-borehole flow testing to define hydraulic connections between fracture zones in bedrock aquifers. *J Appl Geophys* 30:261–279
- Paillet FL (2000) A field technique for estimating aquifer parameters using flow log data. *Ground Water* 38(4):510–521
- Perrin J, Mascré C, Massuel S et al (2009) Tank management in Andhra Pradesh, India: percolation vs. irrigation. *IAHS Publication* 330, IAHS, Wallingford, UK, pp 28–33
- Perrin J, Mascré C, Pauwels H, Ahmed S (2011) Solute recycling: an emerging threat to groundwater resources in southern India? *J Hydrol* 398:144–154. doi:10.1016/j.jhydrol.2010.12.024
- Reddy DV, Nagabhushanam P, Sukhija BS, Reddy AGS (2009) Understanding hydrological processes in a highly stressed granitic aquifer in southern India. *Hydrol Process* 23:1282–1294. doi:10.1002/hyp.7236
- Rushton KR (2003) *Groundwater Hydrology: conceptual and computational models*. Wiley, England, 416 pp
- Sander P (2007) Lineaments in groundwater exploration: a review of applications and limitations. *Hydrogeol J* 15(1):71–74
- Sander P, Minor TB, Chesley MM (1997) Groundwater exploration based on lineament analysis and reproducibility tests. *Ground Water* 35:888–894
- Silliman S, Robinson R (1989) Identifying fracture interconnections between boreholes using natural temperature profiling: I. conceptual basis. *Ground Water* 27(3):393–402
- Taylor R, Howard K (2000) A tectono-geomorphic model of the hydrogeology of deeply weathered crystalline rock: evidence from Uganda. *Hydrogeol J* 8(3):279–294
- Wright EP (1992) The hydrogeology of crystalline basement aquifers in Africa. *Geol Soc Spec Publ* 66:1–27
- Wyns R, Baltassat JM, Lachassagne P, Legchenko A, Vairon J, Mathieu F (2004) Application of SNMR soundings for groundwater reserves mapping in weathered basement rocks (Brittany, France). *Bull Soc Geol Fr* 175(1):21–34
- Zaidi FK, Ahmed S, Maréchal JC, Dewandel B (2007) Optimizing a piezometric network in the estimation of the groundwater budget: a case study from a crystalline-rock watershed in southern India. *Hydrogeol J* 15:1131–1145